

# Charged-particle induced radioluminescence of copper-halide perovskite films and detector assemblies for spaceborne measurements

Mátyás Hunyadi

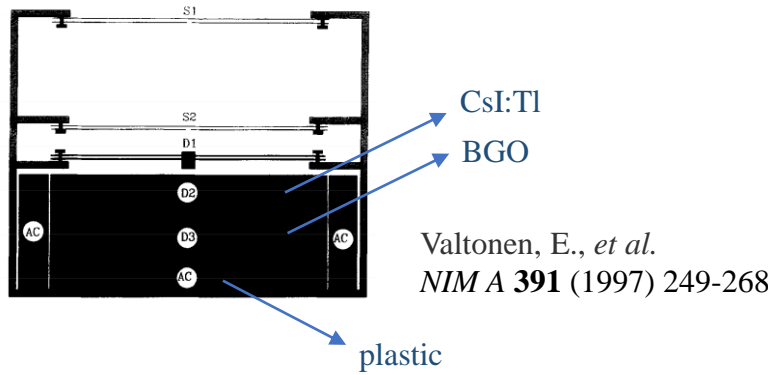
*Institute for Nuclear Research, Debrecen, Hungary*



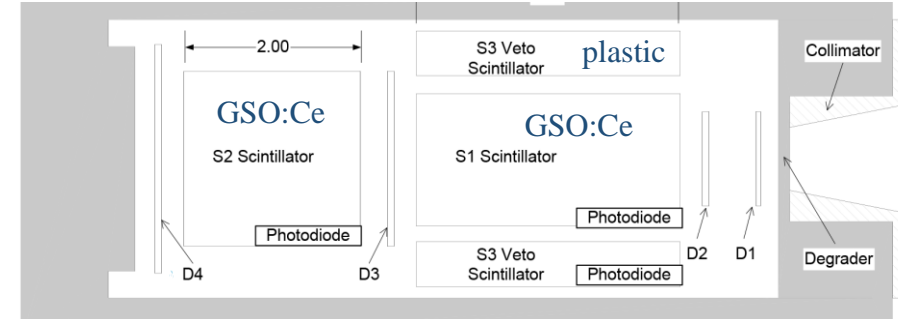
ASAPP 2023, Perugia, 23 June 2023

# Scintillators in space missions

SOHO mission – HED instrument

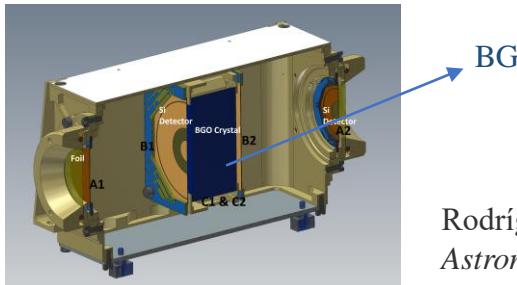


DSX Spacecraft – High Energy Proton Telescope (HEPS)



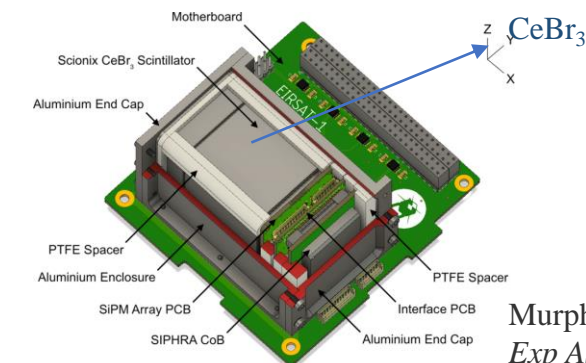
Dichter, B.K., et al.  
*Proc. of SPIE Vol. 7438*, 743806  
Redus, R.H., et al.  
*NIM A* **482** (2002) 281–296

Solar Orbiter – High Energy Telescope (HET)



Rodríguez-Pacheco, J., et al.  
*Astronomy & Astrophysics* **642**, A7 (2020)

CubeSat – EIRSAT-1

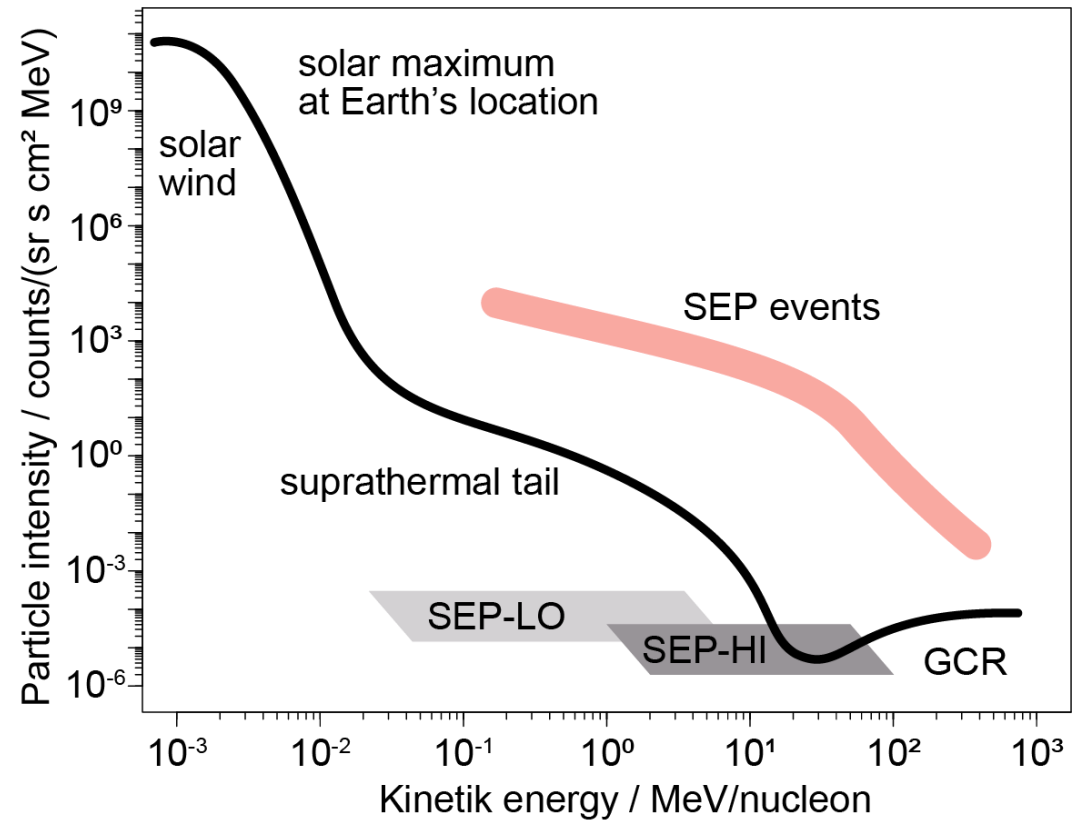


Murphy, D., et al.  
*Exp Astron* **52**, 59–84 (2021)

# Scintillators in space missions

## SEP regions

- Low-energy part  
TOF technique  
MCPs + SSDs
- High-energy part  
Energy-loss technique  
SSDs + bulk scintillators
- Mid-energy part  
Combined technique  
Thin-film + bulk scintillators + SSDs



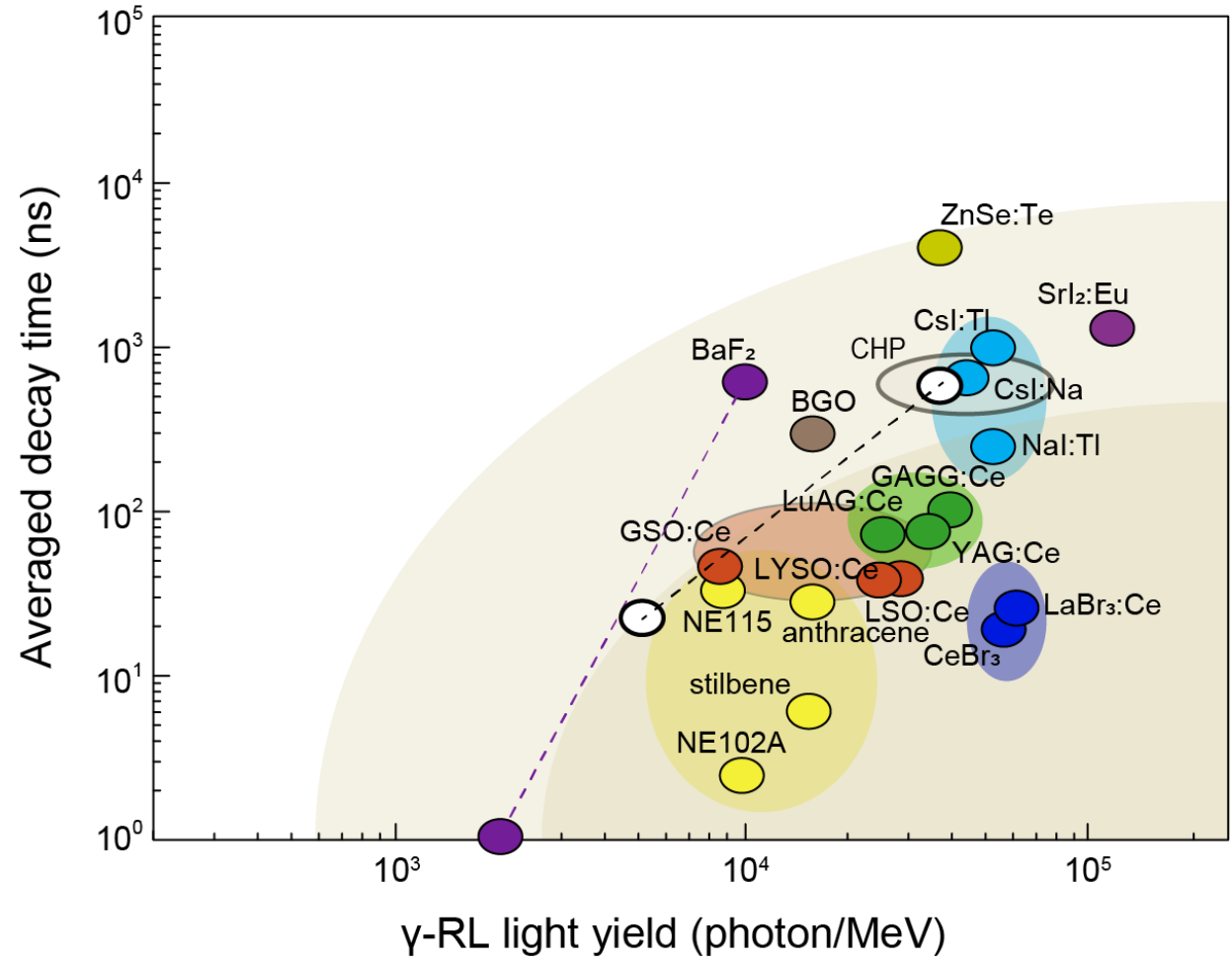
# Scintillator landscape

## Basic requirements

- High light yield
- Short decay time
- High purity single crystals
  - Transparency
  - Minimize defect states
- Linear energy conversion
  - Energy resolution
- Afterglow-free

## Limiting factors

- Hygroscopic
- Radiation sensitive
- Temperature sensitive
- Internal radioactivity



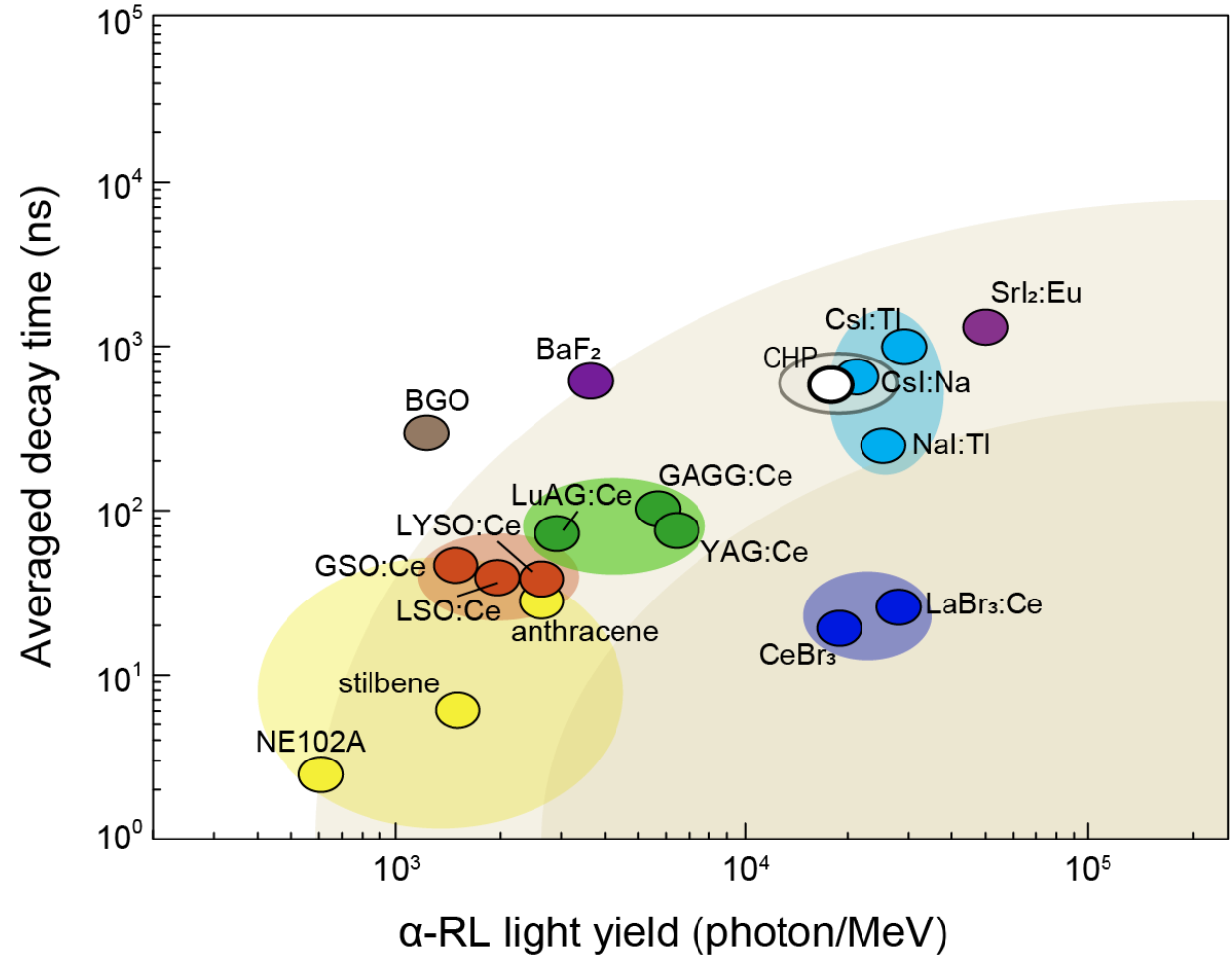
# Thin-layer scintillators

## Limiting factors

- Hygroscopicity
- Radiation sensitivity
- Temperature sensitivity
- Internal radioactivity
- Strong recoil quenching
- Brittleness, fracturing



- intrinsic scintillator
- non-hygroscopic
- polycrystalline
- (blue emitter)



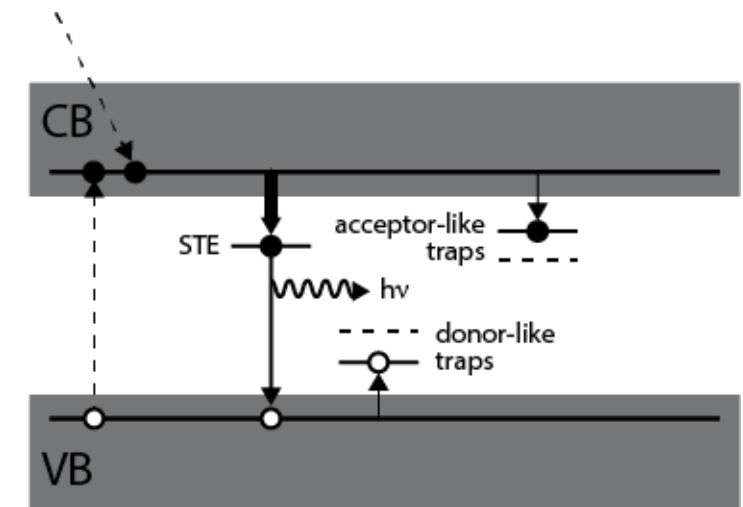
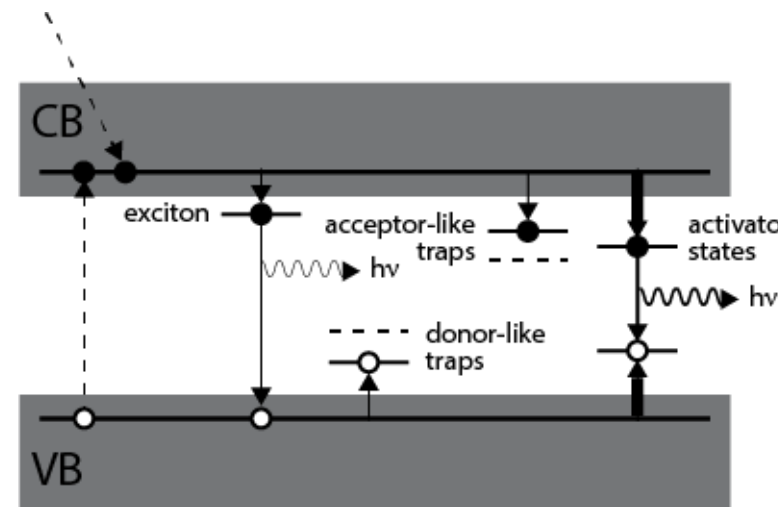
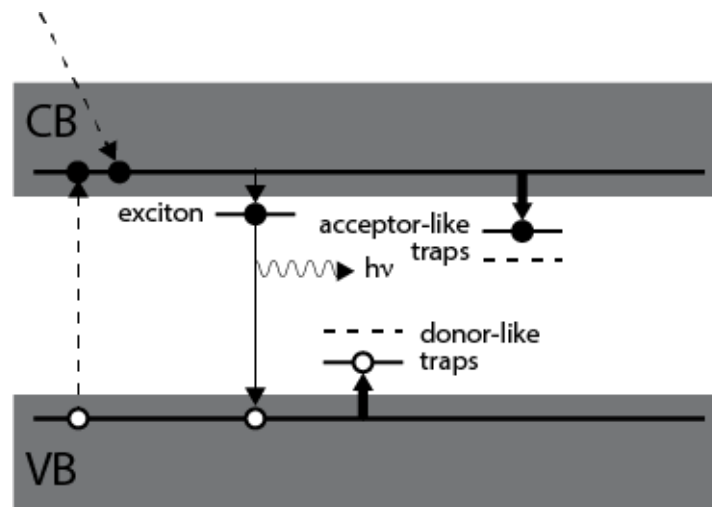
# Polycrystalline scintillators

Offers

- Sufficient stability and flexibility
- Simple and cheap production technology
- Unlimited sensing surface

Requires

- Defect tolerant electronic structure
- Deeply bound excitons



# Perovskite structure

General composition:  $\text{ABX}_3$

Octahedral compartments

Highly ionic crystal

- large displacement energies
- shallow vacancy states

Band edge formation

Low exciton binding energy

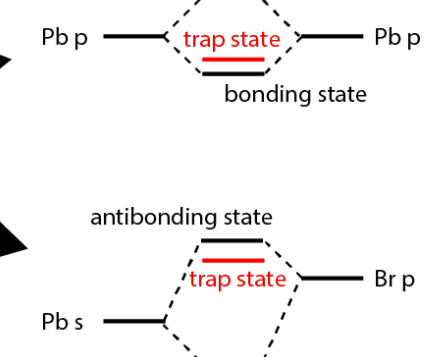
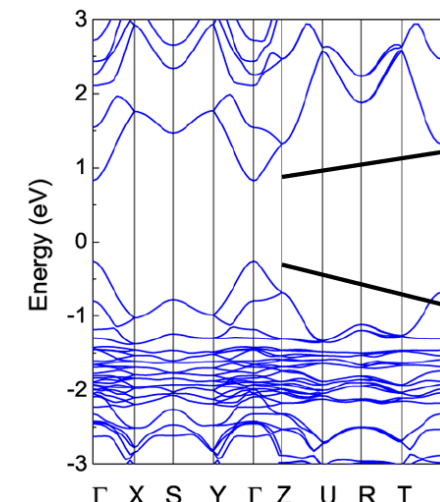
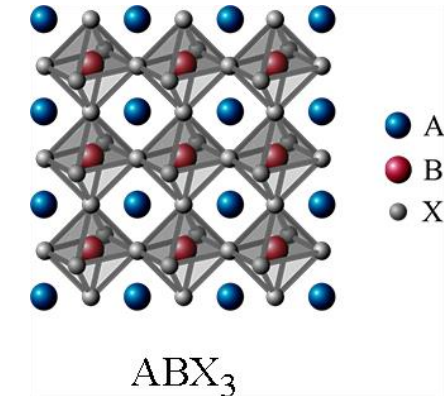
Best studied composition:  $\text{CsPbBr}_3$

Red arrow → Replacement of Pb  
Prone to decomposition

Kojima A., et al.,  
*Am. Chem. Soc.* 2009, 131, 6050–6051

$$t = \frac{r_A + r_X}{\sqrt{2}(r_B + r_X)}$$

Goldschmidt  
tolerance factor



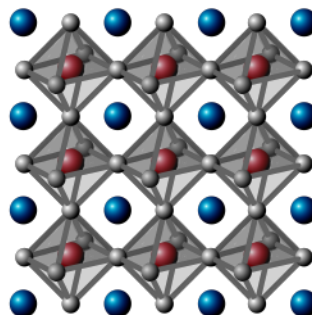
Kang J., Wang LW.  
*J. Phys. Chem. Lett.* 2017, 8, 489–493

# Perovskite-analogue compositions

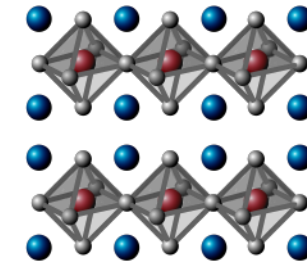
Exciton binding energy

Electronic dimensionality

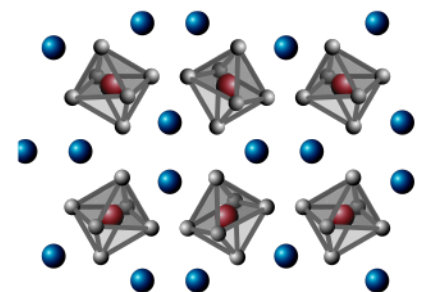
Low-D crystal → High BE



3D



1D/2D



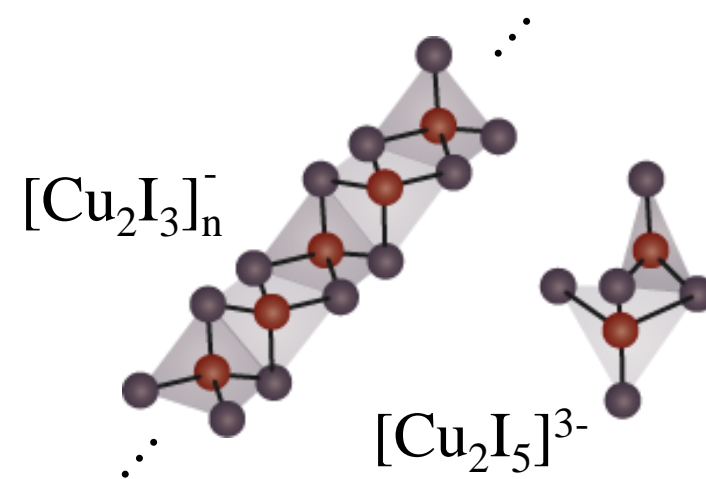
0D

True perovskites vs. Perovskite-analogues

Examples of luminescent low-D perovskites:



CCX



→ Self-trapped excitons (STE)

# Photoluminescence

Blue emission

440 nm

Large Stokes-shift

132 nm

Optical attenuation length

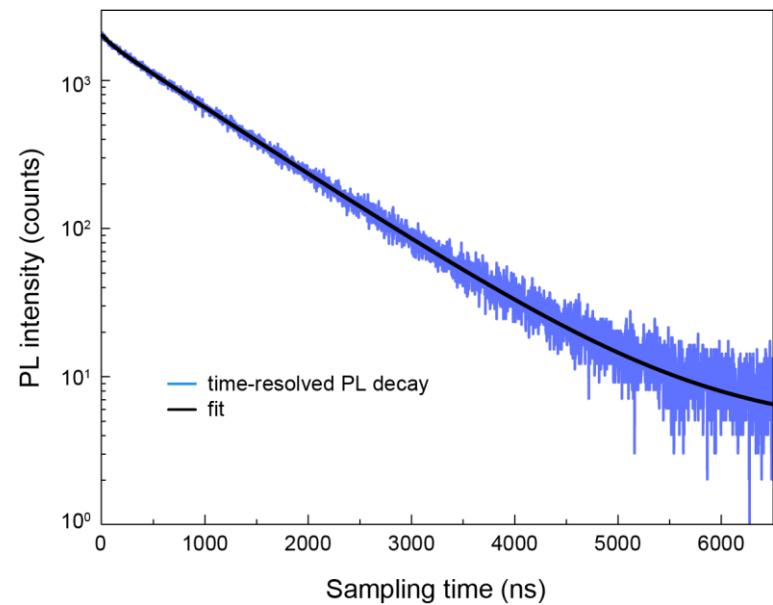
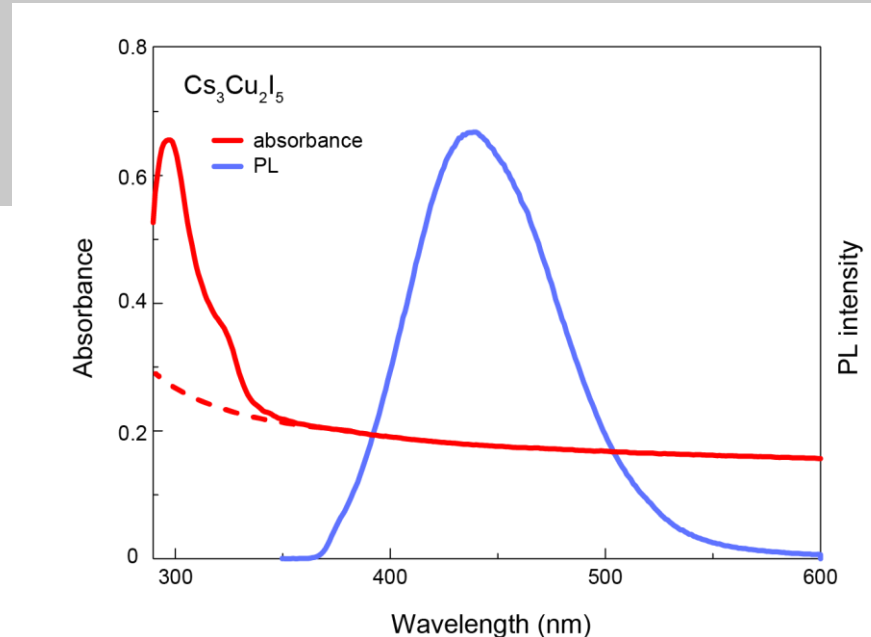
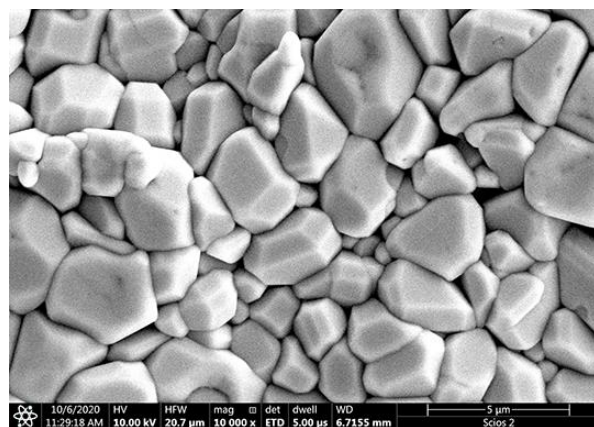
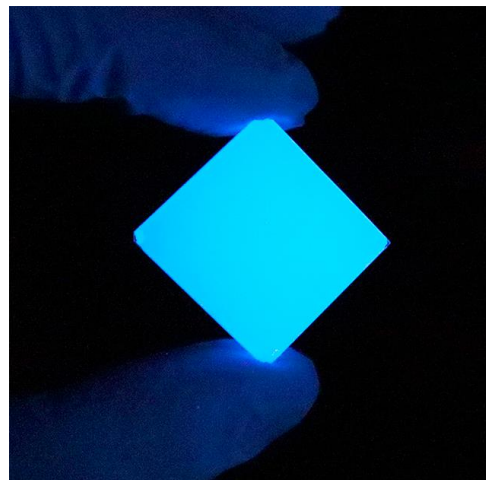
~1.4 mm

PLQY

71 %

Decay time

950 ns



# Radioluminescence systematics

RL response characterization

- Protons,  $\alpha$ -particles, heavy ions, (electrons)
- Temperature dependence
- Timing accuracy and test experiments

Comparison to conventional scintillators

Radiation hardness

Detector design

- Stopping layers
- Non-stopping layers, PoC telescope prototype

Development concept and outlook ...

# Radioluminescence waveform

Time resolved RL emission

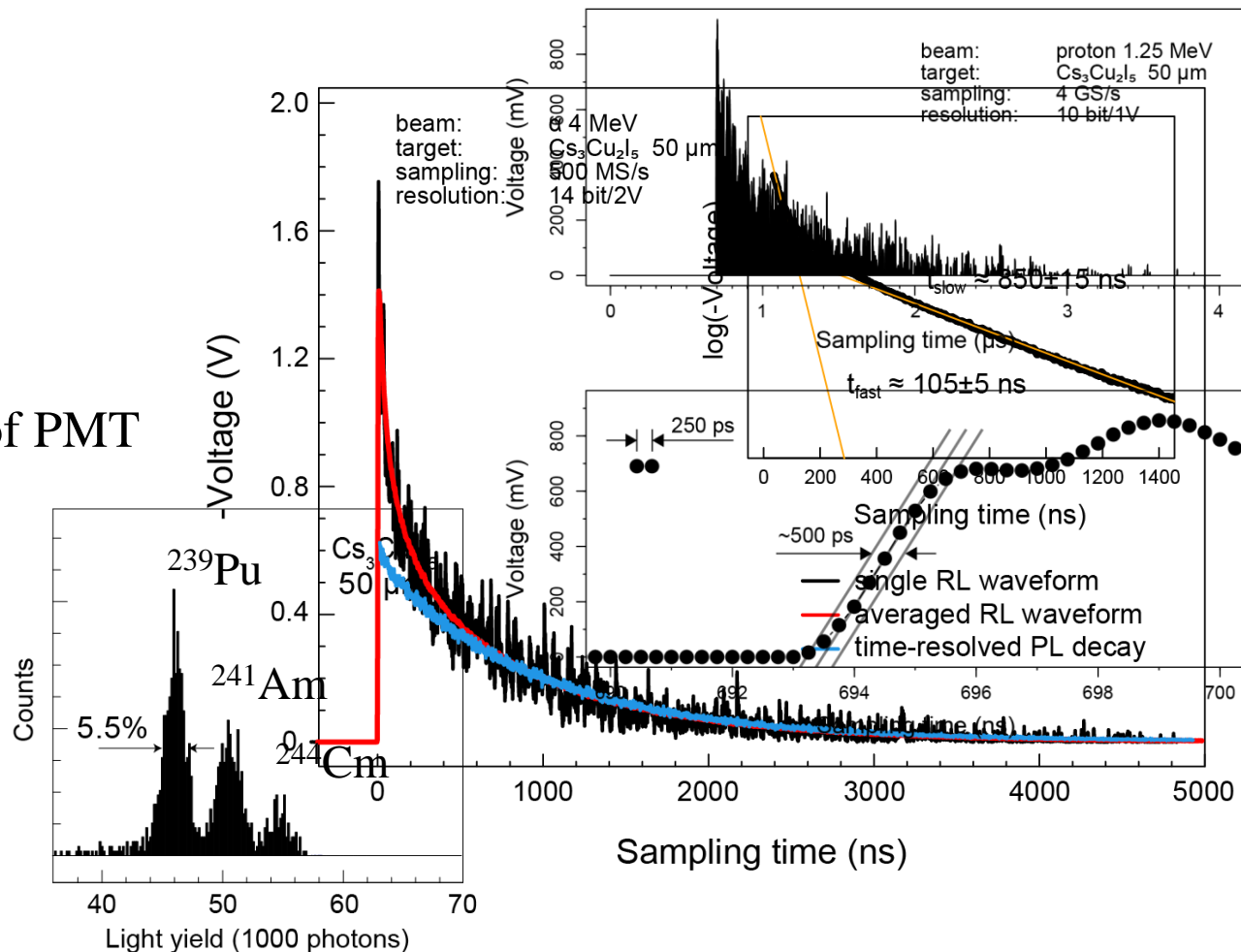
Multiexponential decay character

- Fast component       $\sim 100$  ns (10 %)
- Slow component       $\sim 850$  ns (90 %)

Pulse front is shaped by the transit-time jitter of PMT

Energy resolution  $\sim 5.5\%$  FWHM

No phosphorescence (afterglow)

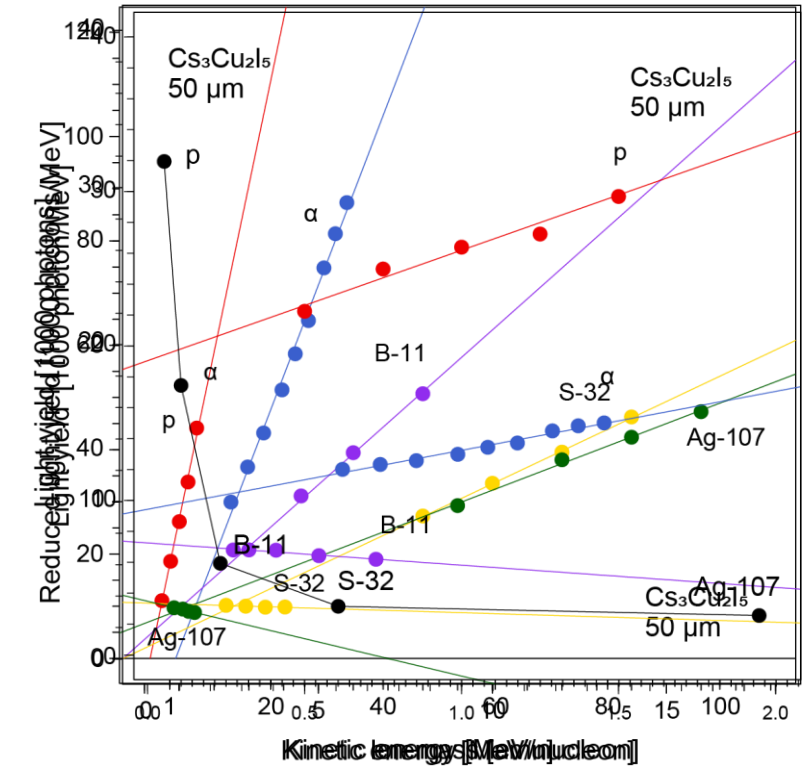
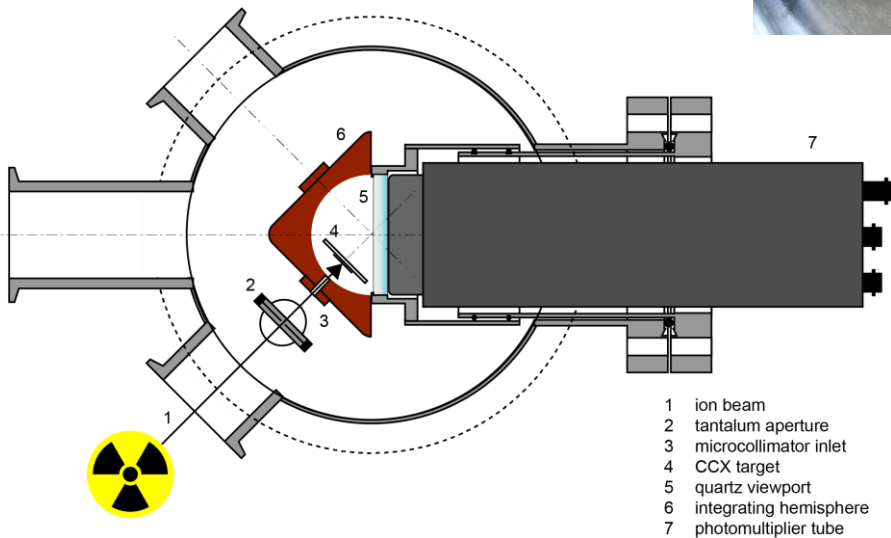


# Heavy-ion radioluminescence

Absolute light yield measurement  
Integrating sphere setup

Ligh yields:

- Protons: 31900 ph/MeV
- Alphas: 17400 ph/MeV



→ Luminescence quenching

# Heavy-ion radioluminescence

Quenching effect, non-linear excitation-density dependence of luminescence yield

Birk's law

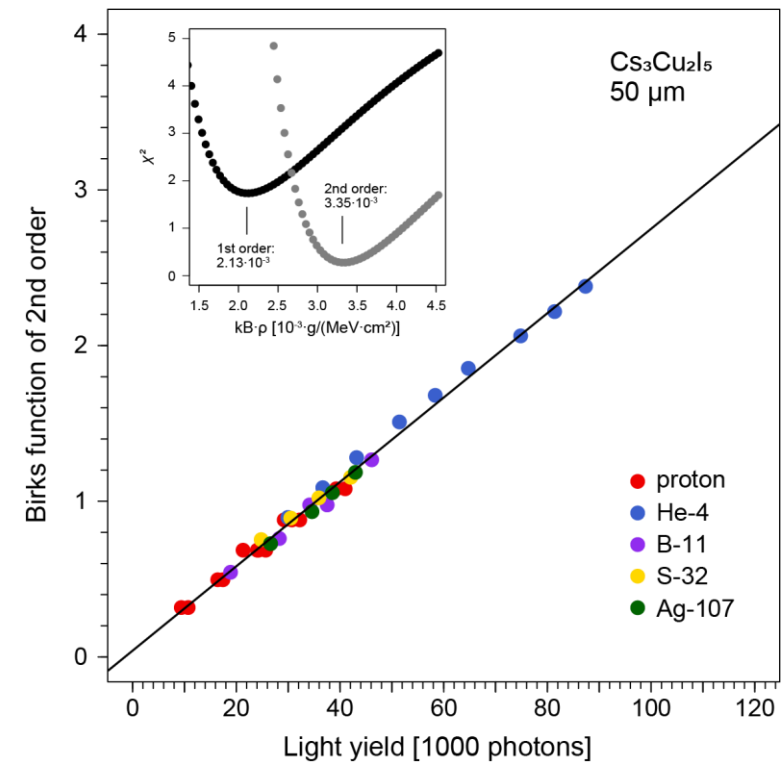
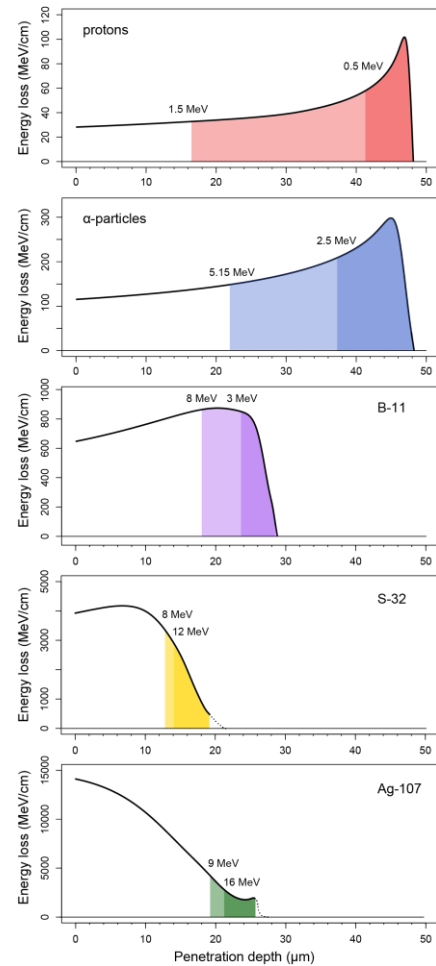
$$L = S \int_{x=0}^{x_{SR}} \frac{\frac{dE}{dx}}{1 + kB \frac{dE}{dx} + C \left( \frac{dE}{dx} \right)^2}$$

Energy range tested: 0.1-1 MeV/nucleon

$$kB \cdot \rho = 2-3 \cdot 10^{-3} \text{ g/(MeV} \cdot \text{cm}^2)$$

Birk's const.	$\text{Cs}_3\text{Cu}_2\text{I}_5$	GAGG(Ce)	$\text{CsI}(\text{Tl})$	NE102A
$kB \cdot \rho$ $10^{-3} \text{ g/(MeV} \cdot \text{cm}^2)$	2-3 <i>this work</i>	6.5	2-3	>20

[Furuno-2021] [Tretyak-2010] [Ogawa-2010]



Weak saturation effect

# Comparison to commercial scintillators

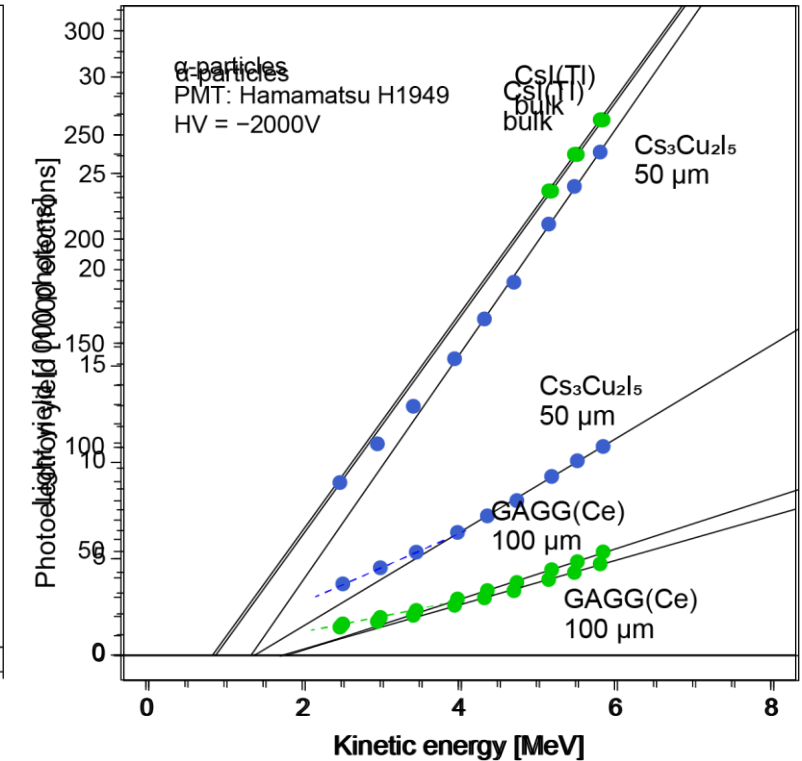
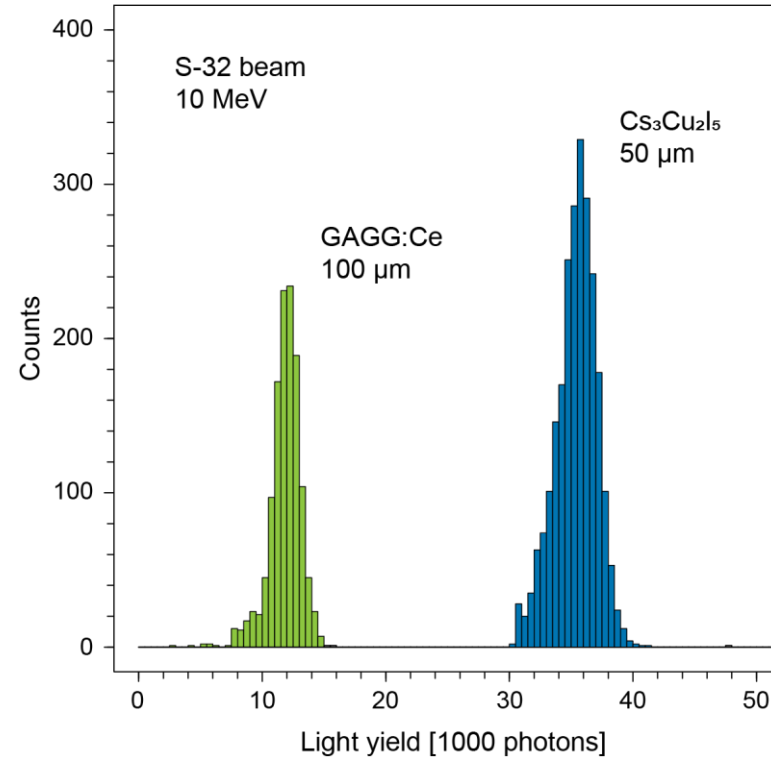
GAGG:Ce and CsI:Tl

Extremes of stability and light yield

Light yield ratio

$$R = LY(\text{Cs}_3\text{Cu}_2\text{I}_5)/LY(\text{GAGG:Ce})$$

- For protons: 1.6
- For S-32 beam: 3.0

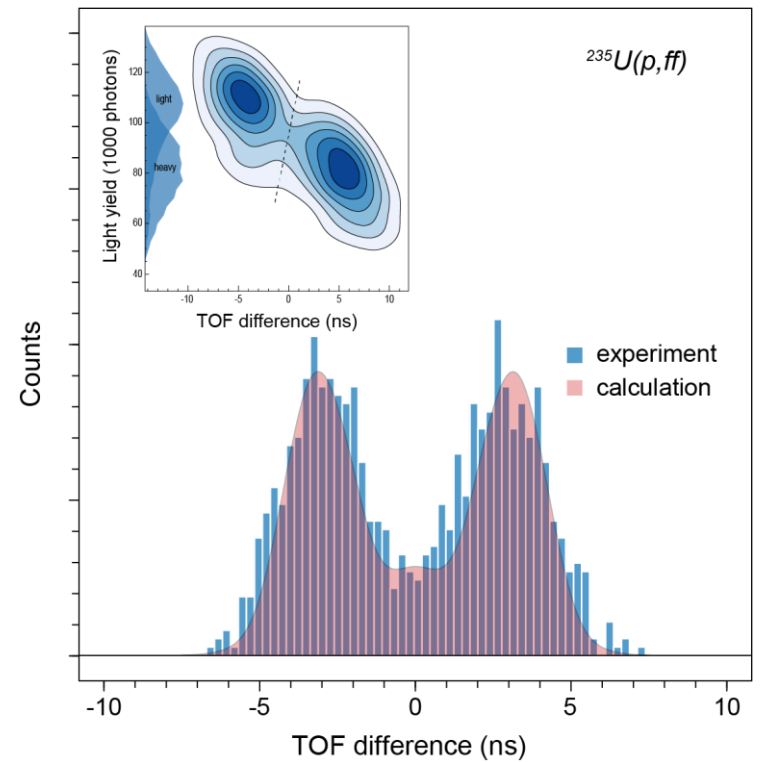
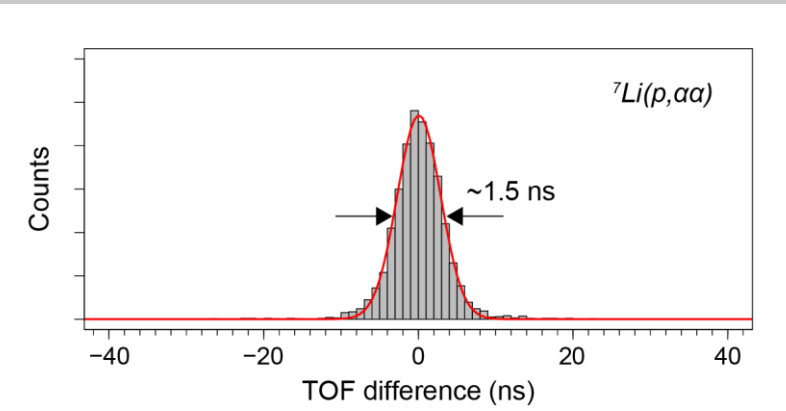
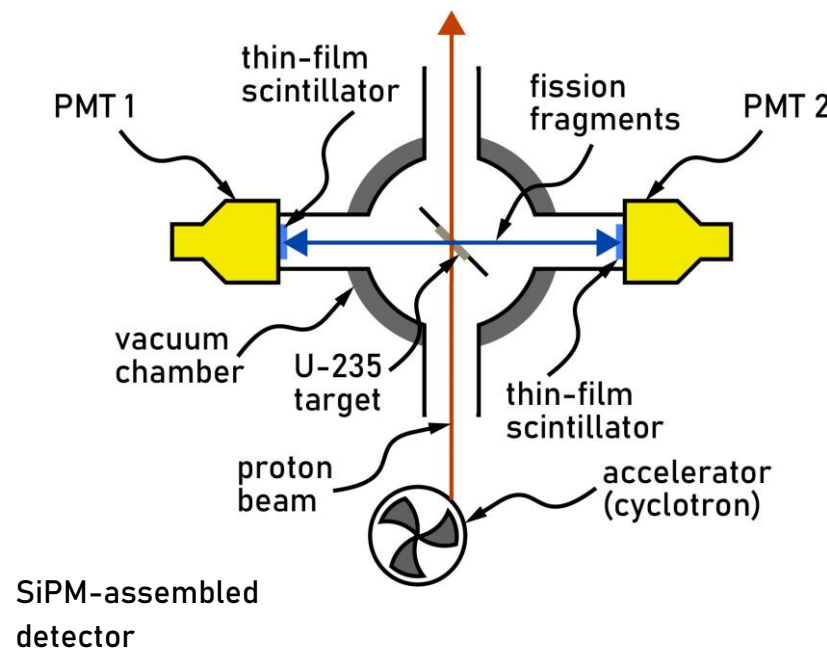


# Test experiments for timing accuracy

Nuclear fission in time coincidence mode

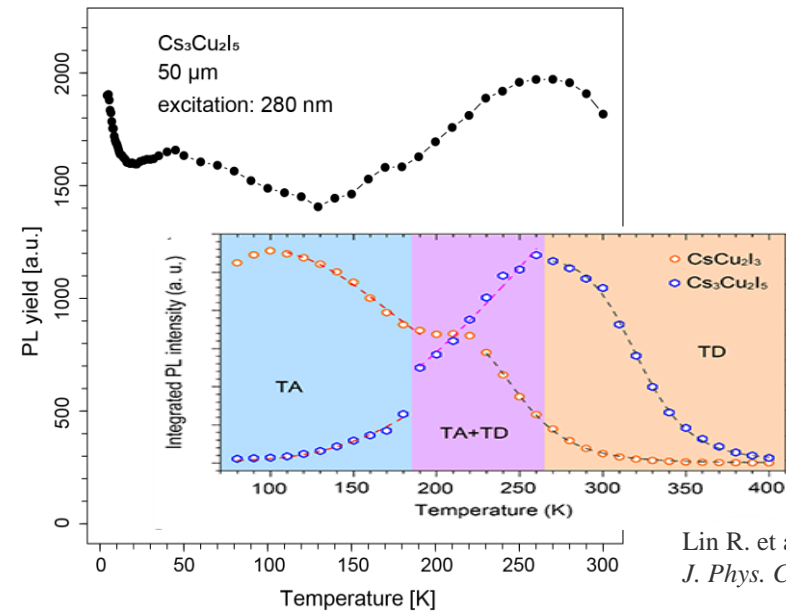
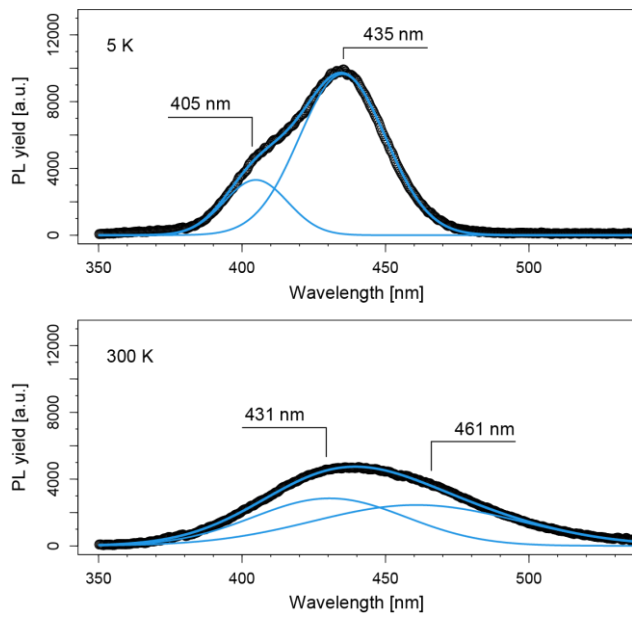
Method: TOF + spectroscopy

- Double- $\alpha$  decay of  $^{8}\text{Be}^*$
- $^{235}\text{U}$  fission with typical mass distribution

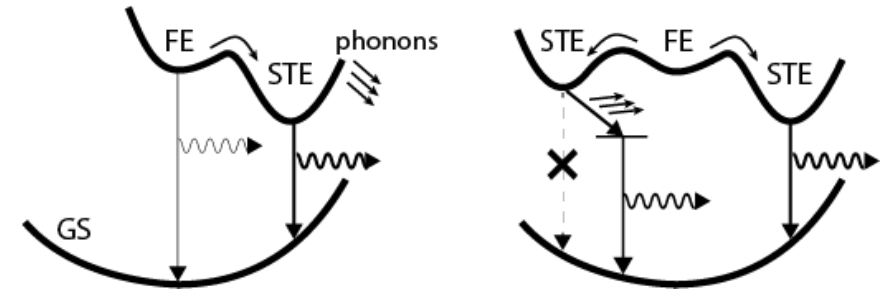


# Temperature dependence

Photoluminescence:  $Y_{PL}(T)$   $T=4.2\text{ K}$  to  $RT$   
Excitation: 280 nm

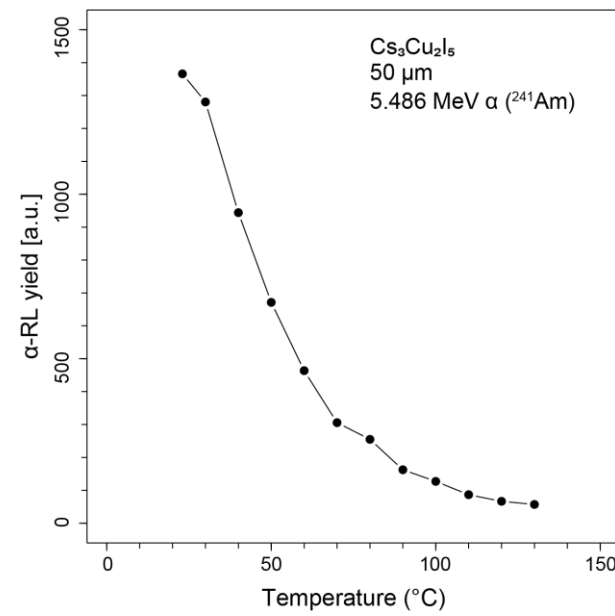
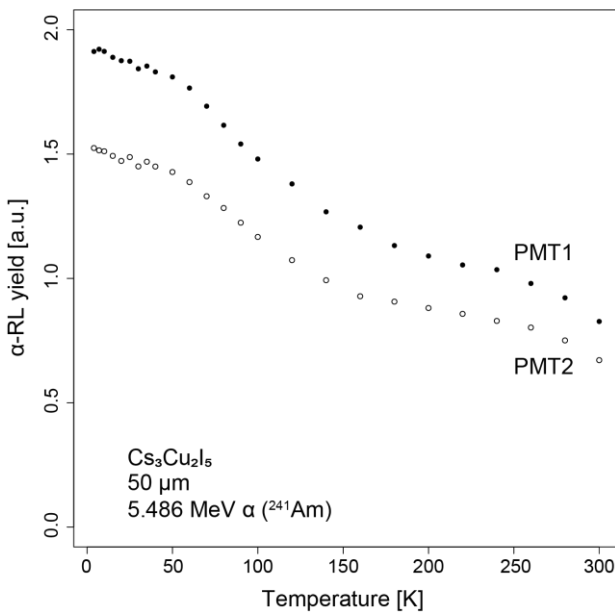


Thermal detrapping  $> 250\text{ K}$   
Phonon-assisted emission  $120\text{--}250\text{ K}$   
Free excitons  $< 20\text{ K}$

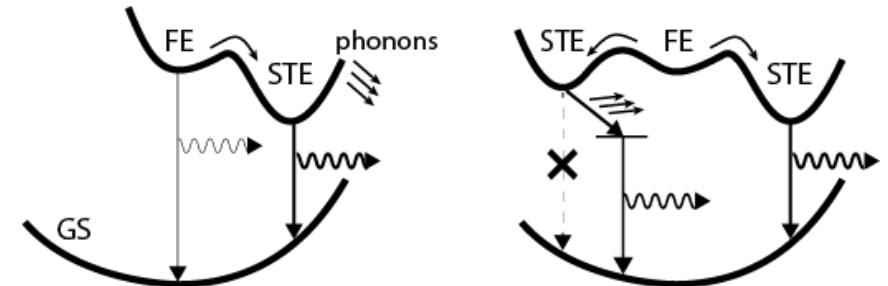


# Temperature dependence

$\alpha$ -radioluminescence:  $Y_{\alpha\text{-RL}}(T)$   $T=4.2 \text{ K to } 400 \text{ K}$   
Monotonic behaviour in contrast to PL



Thermal detrapping  $> 250 \text{ K}$   
Phonon-assisted emission  $120-250 \text{ K}$   
Free excitons  $< 20 \text{ K}$



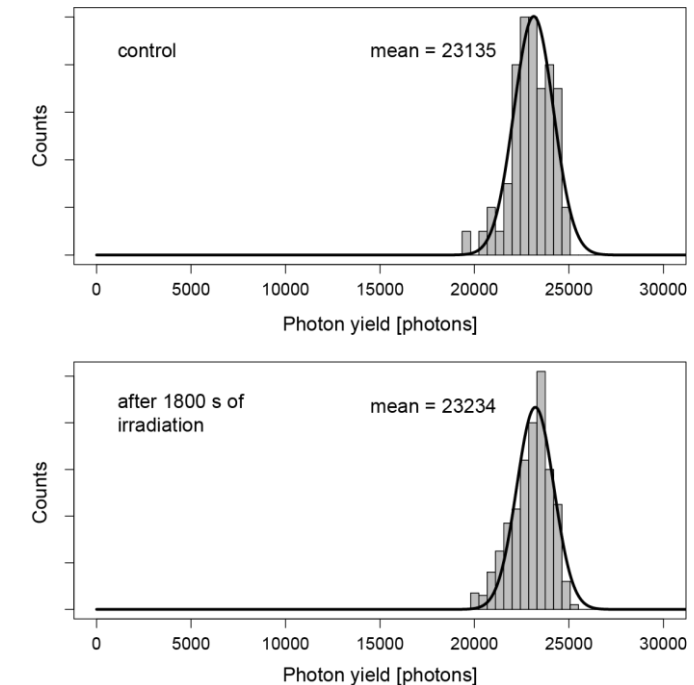
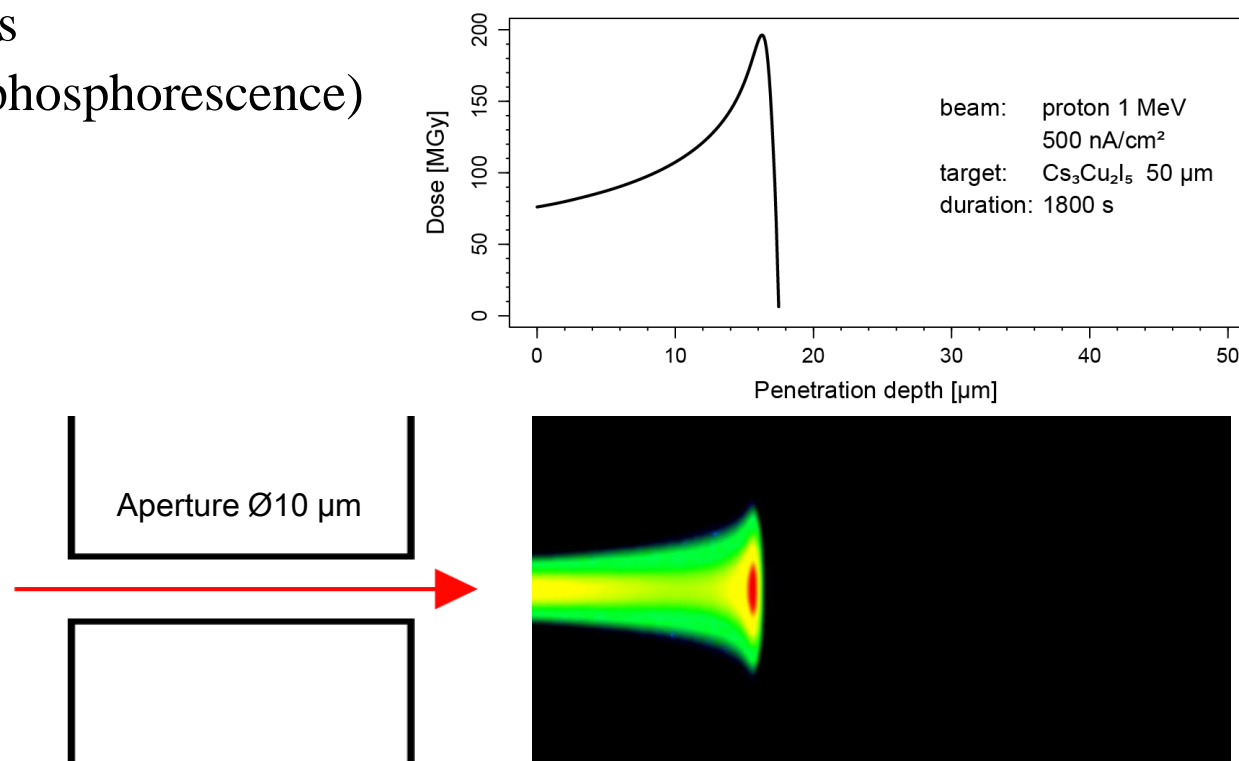
Polaron dynamics at high excitation density  
Frenkel-pair relaxation  
Deep trap states

# Radiation hardness

Differential radiation damage

Identical probe and irradiation volumes

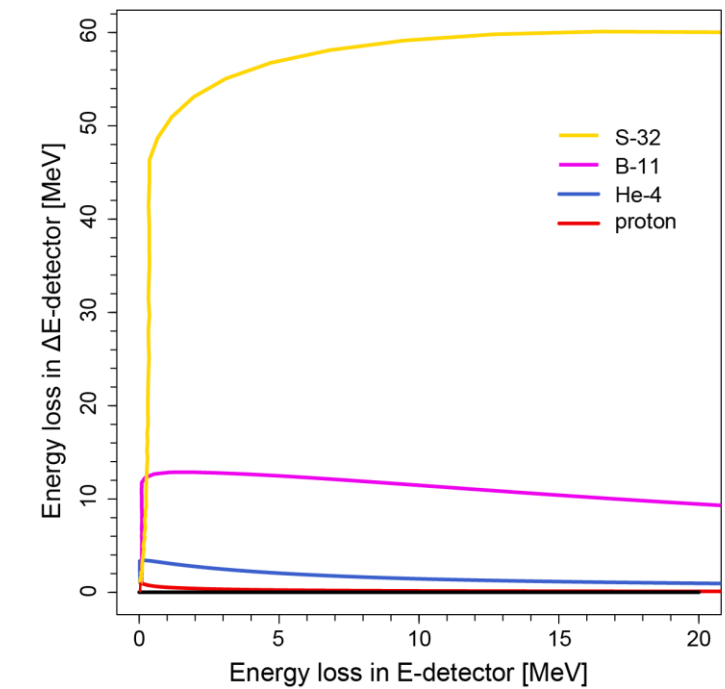
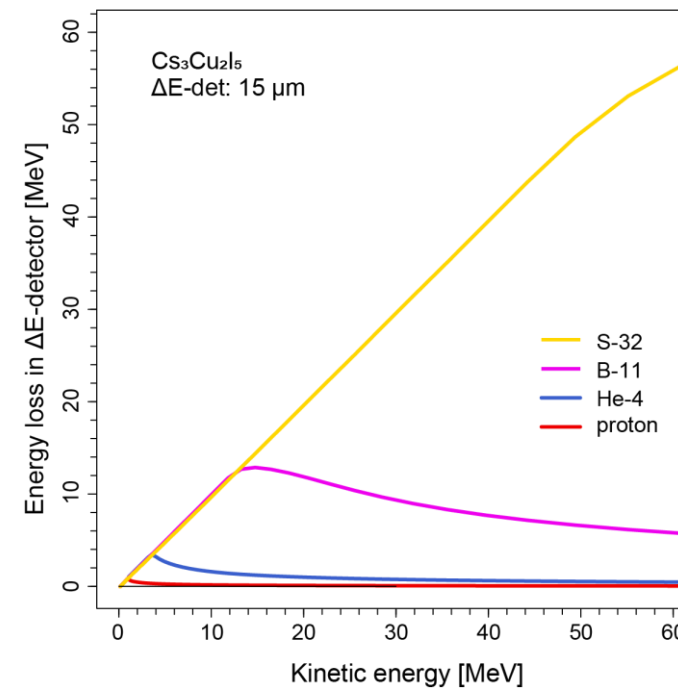
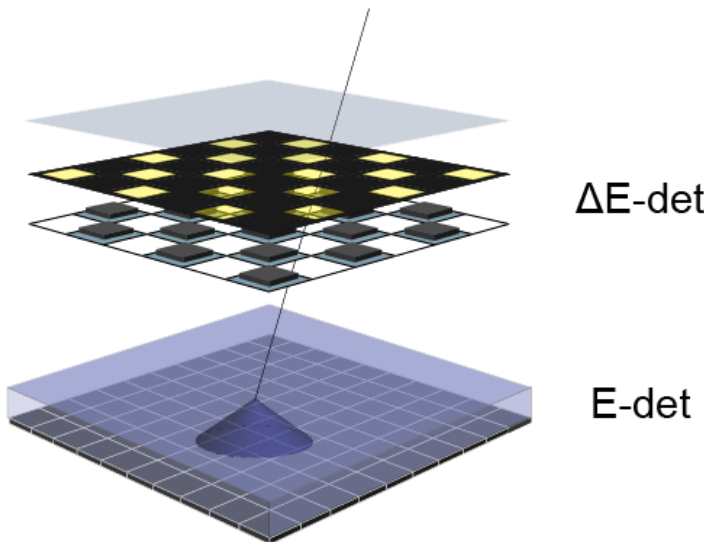
- Luminescence yield
- Color centers
- Afterglow (phosphorescence)



# Telescope concept

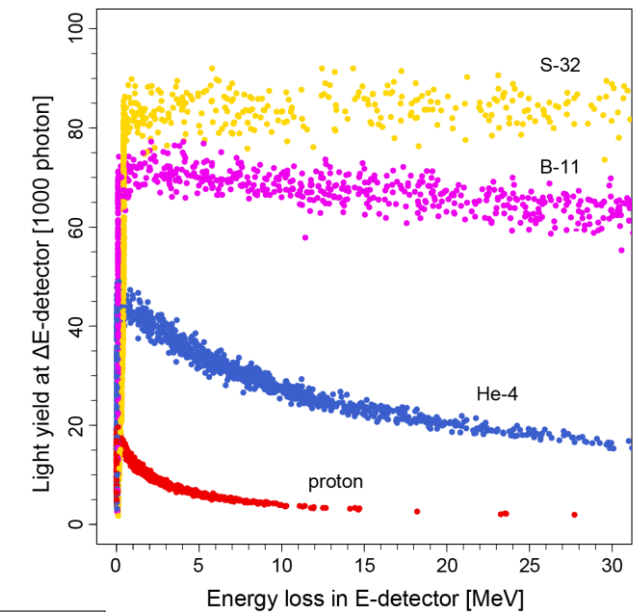
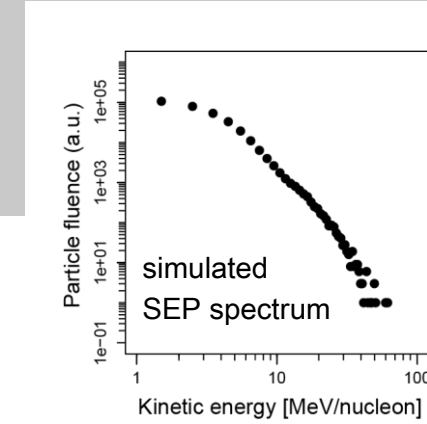
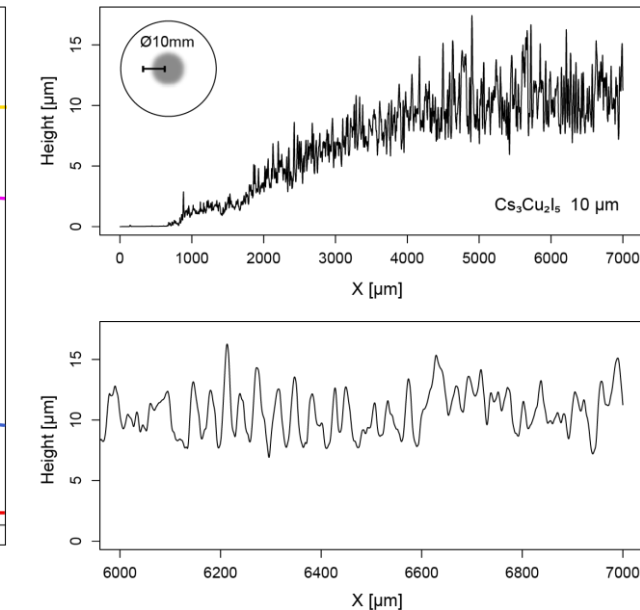
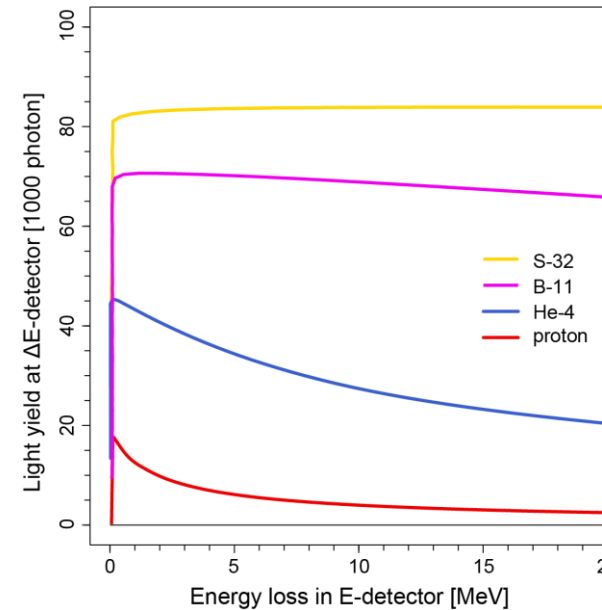
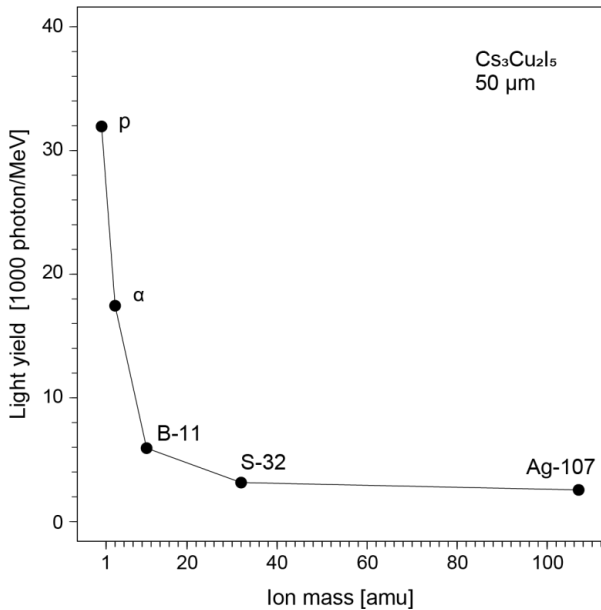
Thin-layer scintillators for particle telescopes

Critical thickness: energy vs mass  
Thickness uniformity  
Geometric efficiency of light collection



# Telescope concept

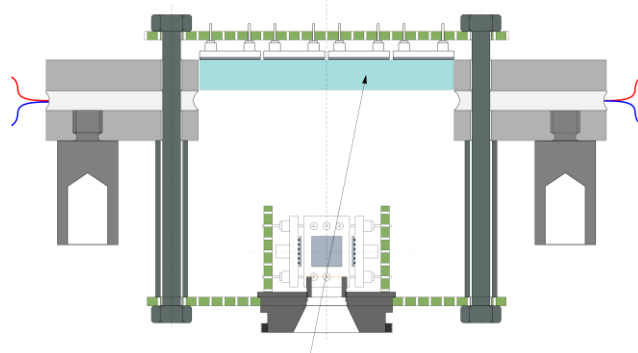
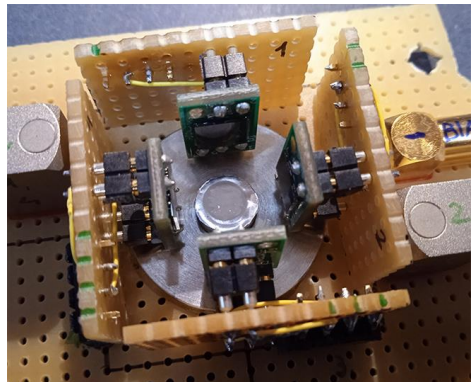
Quenching: loss of dispersion for heavy ions  
Decreased dynamic range for light measurement  
Layer uniformity



# PoC prototype

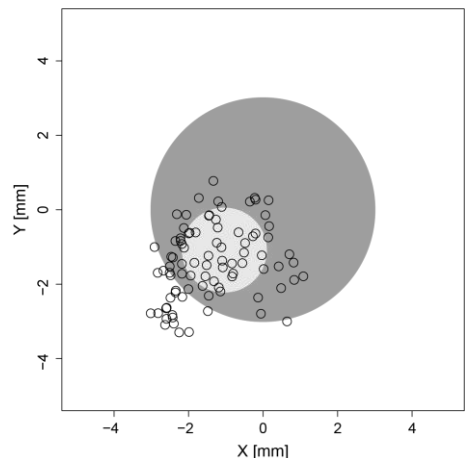
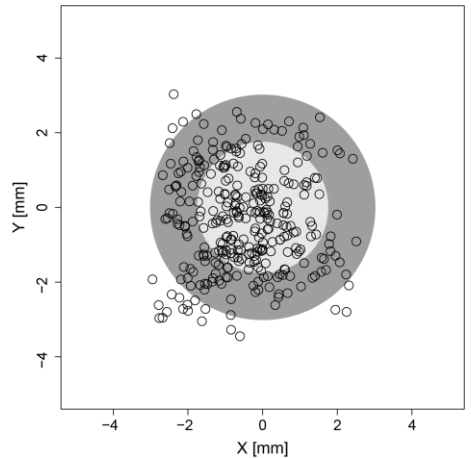
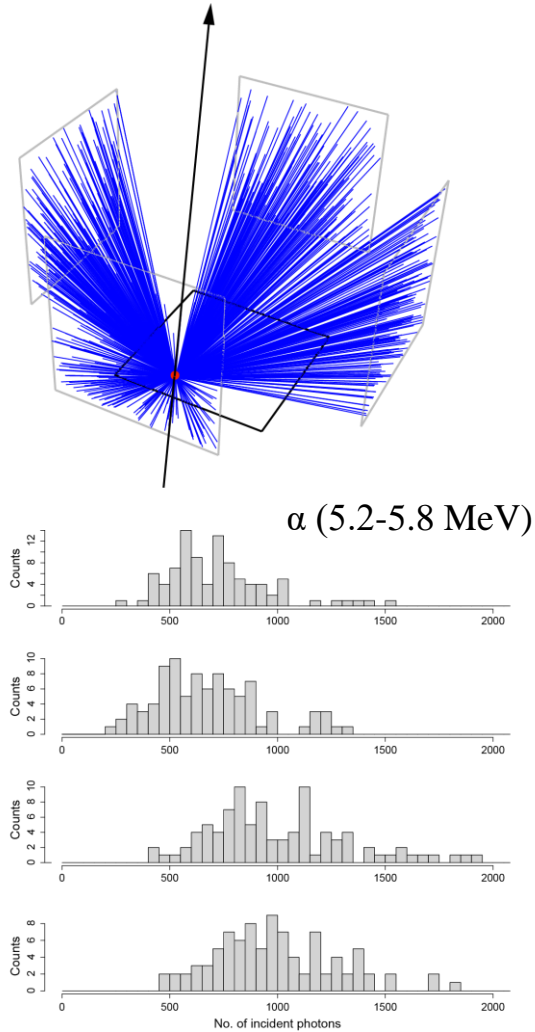
$\Delta E$ -detector design:

- Layer:  $\text{Cs}_3\text{Cu}_2\text{I}_5$  15  $\mu\text{m}$
- Substrate: Al-Mylar 5  $\mu\text{m}$
- Readout: 4 SiPMs, effective solid angle: 13%



E-detector design:

- Stopping layer: BGO/LSO(Ce) 6 mm
- Readout: SiPM-tile



# Development concept and outlook

Extension to higher energy beams of heavy ions

Temperature and ion mass systematics

Layer quality (stability, homogeneity)

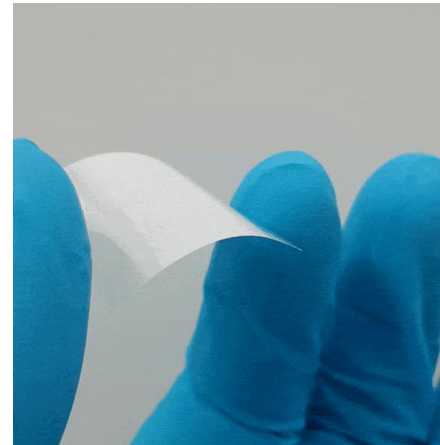
Prototype telescopes tests with accelerated beams

Electron-RL, Compton-coincidence measurements

Testing and improving mass-resolving power

Fully transparent layers, single crystals,  $\gamma$ -ray detection

Development of read-out for position sensitivity



# The team and the technical background



Mátyás  
Hunyadi



Gergely  
Samu



Lóránt  
Csige



Csaba  
Janáky



Attila  
Csík



Cintia  
Hajdú

**Synthesis and characterization**  
Univ. of Szeged (SZTE)  
Dept. Of Physical Chemistry and Materials Science



**Accelerator facilities**  
Inst. for Nuclear Research  
(ATOMKI)



*Tandetron linear  
accelerator*

**Radiation sources**  
**Cryophysics**  
**Nuclear electronics**  
**Ion beam physics**  
**Surface technologies**



**Surface and  
structural analytics:**  
SEM-STEM FIB  
SIMS/SNMS  
STM - XPS  
XRD  
UVVIS, TRPL, UPS

